

RIGA TECHNICAL UNIVERSITY

Janis KANDIS

**NEW METHOD FOR QUALITY INSPECTION OF
EXTRUSION WELDING**

The summary of PhD Thesis

Field: Mechanical Engineering

Sub-field: Mechanical Engineering Technology

Riga 2013

RIGA TECHNICAL UNIVERSITY

The Faculty of Transport and Mechanical Engineering

Institute of Mechanical Engineering Technologies

Janis KANDIS

PhD candidate at programme "Apparatus Engineering"

**NEW METHOD FOR QUALITY INSPECTION OF
EXTRUSION WELDING**

The summary of PhD Thesis

Field: Mechanical Engineering

Sub-field Mechanical Engineering Technology

Supervisor of research:

Dr. sc. ing., Assistant Professor

N.MOZGA

Riga 2013

UDK 621.9.08

Kandis J. Jauna metode ekstrudēto
šuvju kvalitātes pārbaudei.
Promocijas darba kopsavilkums.-
R.:RTU, 2012.-35 lpp.

Iespiests saskaņā ar MTI institūta 2012. gada
30. augusta lēmumu, protokols Nr.5.



This work has been supported by the European Social Fund within the project «Support for the implementation of doctoral studies at Riga Technical University».

PROMOCIJAS DARBS IZVIRZĪTS INŽENIERZINĀTŅU DOKTORA GRĀDA IEGŪŠANAI RĪGAS TEHNISKAJĀ UNIVERSITĀTĒ

Promocijas darbs inženierzinātņu doktora grāda iegūšanai tiek publiski aizstāvēts 2013. gada....., plkst. Rīgas Tehniskās universitātes Transporta un mašīnzinību fakultātē, Ezermalas ielā 6,auditorijā.

OFICIĀLIE RECENZENTI

Prof. Juris Krisbergs

Rīgas Tehniskā Universitāte, Latvija

Prof. Zbigniew Zimniak

Wrocław University of Technology, Polija

Prof. Dijs Sergejevs

Rīgas Tehniskā Universitāte, Latvija

APSTIPRINĀJUMS

Apstiprinu, ka esmu izstrādājis doto promocijas darbu, kas iesniegts izskatīšanai Rīgas Tehniskajā universitātē inženierzinātņu doktora grāda iegūšanai. Promocijas darbs nav iesniegts nevienā citā universitātē zinātniskā grāda iegūšanai.

Jānis Kandis(Paraksts)

Datums:

Promocijas darbs ir uzrakstīts angļu valodā, satur 4 nodaļas, secinājumus, izmantoto informācijas avotu sarakstu, 53 attēlus, kopā 108 lapaspuses. Literatūras sarakstā ir 66 informācijas avoti. Pievienoti 3 pielikumi.

TABLE OF CONTENTS

GENERAL DESCRIPTION OF PROMOTION THESIS	7
Topicality of Subject.....	7
Objective and Tasks of Thesis	7
Methods of Research	7
Scientific Novelty	8
Main Research Results.....	8
Practical Application.....	8
In this thesis the author presents	8
Approbation of Thesis	8
Publications.....	9
Structure and Volume of Thesis	9
1. BASIC CONCEPT OF PROBLEM.....	10
1.1. Extrusion.....	10
1.2. Testing methods of extrusion welding joints in the extrusion process.....	11
1.3. Defination of problem.....	12
1.4. Conclusions.....	13
2. EXPERIMENTAL STUDY AND FEM-MODELLING OF SHEARING PROCESS ..	14
2.1. Introduction.....	14
2.2. Experimental work.....	14
2.3. FEM-model of the shearing process	15
2.4. Results of the FEA	16
2.6. Conclusions.....	18
3. ANALYSIS OF GAS POCKET FORMATION DURING EXTRUSION OF AL PROFILES AND ESTABLISHING AN EXTRUSION SEAM WELD LIMIT DIAGRAM .	19
3.1. Introduction.....	19
3.2. Finite Element Models.....	21
3.3. The quality aspects of extrusion welding	21
3.4. Finite Element Models.....	23
3.5. Material Flow in the Weld Chamber	23
3.6. Extrusion form geometrical effect of extrusion welding quality.....	24
3.7. Ternary Extrusion Seam Weld Limiting Diagram.....	26
3.8. Conclusions.....	27
4. DETERMINING THE WELD QUALITY IN EXTRUSION WELDING.....	29
4.1. New innovative concept for testing of extrusion welds.....	29
4.2. Summarization of results	30
4.3. Results analyze of weld testing.....	30
4.3. The mechanics of the new test.....	32
4.4. Conclusions.....	32
CONCLUSIONS AND APPLICATION	34
REFERENCES	35

GENERAL DESCRIPTION OF PROMOTION THESIS

Topicality of Subject

Nowadays, in order to remain competitive in the field of production, metalworking companies are expected to offer the lowest price possible, maintaining flawless quality. The low price level and high quality standard can be achieved only by cutting the labor cost, making production technologies more efficient and establishing new quality testing technologies.

Aluminum has become one of the most progressive metals of the present and future. It is light, solid, not subject to corrosion, easy to process and shape and environmentally friendly, as well as it is recyclable. Since aluminum is widely used in such fields as auto industry, construction of buildings, air transport production, then elimination of the identified casting defects of aluminum has become a requirement of great importance. Such quality tests determine the course and safety of further utilization of profiles.

The currently applied testing technologies for identification of defects in the extrusion welds of aluminum are expensive, time consuming and what is more – they are inaccurate, which results in the loss of time and resources of a company. Therefore it is necessary to develop a more accurate method to replace the current ones and provide more accurate information on the quality of welds of the extruded profiles.

The topicality of the research determines a necessity to develop a quality testing method for inspection of the quality of the extruded welds directly focused on testing the extrusion welding instead of the overall test of the profile, therefore the subject is topical.

Objective and Tasks of Thesis

The objective of the promotion thesis is to develop an accurate and practically usable method for inspection of the extrusion welding of aluminum and identification of defects.

The following tasks were set to accomplish the objective:

1. Analysis and case study of the current quality inspection methods of the extrusion welding;
2. To perform shearing inspection of the aluminum specimen, using the mechanical press, force and stroke measurement indicators;
3. To perform the analysis of development of defects in the extrusion welded joints depending on the geometrical values of the forms;

Methods of Research

In order to accomplish the set objectives and fulfill the given tasks, the following research methods were used during the course of development of the promotion thesis: comparative, analytical and graphical methods. In order to carry out the experimental part, the mechanical presses with capacities of 60 and 2 tons and the extrusion press with a capacity of 180 tons were used. In order to read the experiment data, a force and speed reading indicator was used. The software BLACK CAT[®] was used for data summarization and visualization. The graphical software DEFORM[®] 2D and DEFORM[®] 3D were used for the FEM (Finite element method) and FE-analysis (finite element analysis). Diagrams and figures were used to provide clearness of the research results.

Scientific Novelty

The scientific novelty of the promotion thesis is as follows:

1. A new method for quality inspection of extrusion welding developed to identify defects of the welded joints in the extrusion process;
2. An *extrusion seam weld limit diagram* (ESWLD) was developed to determine the minimum parameters of geometry of the extrusion die's welding chamber.

Main Research Results

The main research results of the promotion thesis are as follows:

It was established that:

1. The current quality inspection methods of extrusion welding do not identify defects of the welded joints;
2. After shearing 1/5 of an aluminum specimen, a crack develops in the specimen. After shearing 3/5 of the aluminum specimen, the effect of the Plateau is observed;
3. The quality of extrusion welded joints depends on the geometry of extrusion forms;
4. A new method for inspection of quality of the welded joints in the extrusion process is developed.

All above mentioned results are a new contribution to the machine science.

Practical Application

The researches carried out in the promotion thesis "New Method for Quality Inspection of Extrusion Welding", compared to the current testing methods, permit focusing the inspection on the welded joints in the extrusion process and provide recommendations for improvement of the extrusion technologies. The method developed is universal.

The developed method permits increasing industrial inspection productivity and since 2012 it is launched in production.

The developed diagram for *extrusion seam weld limit diagram* (ESWLD) provides recommendations to the manufacturers of extrusion dies – to follow the geometrical parameters of extrusion dies.

In this thesis the author presents

1. The quality inspection method of the welded joints in the extrusion process;
2. The practical application of the new method for quality inspection of extrusion welding;
3. The practical application of the geometrical diagram for *extrusion seam weld limit diagram* (ESWLD).

Approbation of Thesis

The main promotion thesis results were presented in the subsequent conferences and seminars with a high level of reputation, receiving approving feedback from the teaching staff of other universities and representatives of the industry:

1. J. Kandis, H.Valberg and Wu Wenbin; "Use of Axisymmetric Shearing as Technological Test Method to gather Flow Stress Data for Metals", AMPT Paris, Oct., 2010;
2. J. Kandis, Wu Wenbin and H. Valberg; "The Mechanics of the Shearing Process studied by FEM-Analysis with Experiments", AMPT Paris, Oct., 2010;
3. J. Kandis, H. Valberg and Wu Wenbin; "On the Mechanics of the Shearing Process in Bar Shearing", ESAFORM Belfast, April, 2011;
4. J. Kandis, H. Valberg and Wu Wenbin; "On the Deformation Mechanism in Shearing with concurrent Crack Growth over the Cut Section", ESAFORM Belfast, April, 2011;
5. J. Kandis, H. Valberg; „Metal flow in two-hole extrusion of Al-alloys studied by FEA with experiments", ESAFORM Germany, March, 2012
6. Henry Valberg, Tony Melkild and Janis Kandis: "Determining The Weld Quality In Extrusion Welding", Italy, 2011;

Publications

There are six scientific articles published on the conducted researches and results and one application for patenting the method submitted:

1. J. Kandis, H.Valberg and W. Wu; „Use of Axisymmetric Shearing as Technological Test Method to gather Flow Stress Data for Metals", Advances in Materials and Processing Technologies, Paris, France, Oct., 2010, pp.352.- 356.;
2. J.Kandis, W. Wu and H. Valberg; "The Mechanics of the Shearing Process studied by FEM-Analysis with Experiments", Advances in Materials and Processing Technologies, Paris, France, Oct., 2010, pp.108.- 112.;
3. J.Kandis, H. Valberg and W. Wu; „On the Mechanics of the Shearing Process in Bar Shearing", Submitted to: European Scientific Association for Material Forming, Belfast, United Kingdom, April, 2011, pp.615.- 620.;
4. J.Kandis, H. Valberg and W. Wu; „On the Deformation Mechanism in Shearing with concurrent Crack Growth over the Cut Section", European Scientific Association for Material Forming, Belfast, United Kingdom, April, 2011, pp.615.– 620.;
5. J. Kandis, H. Valberg, T. Melkild; „Determining the Weld Quality in Extrusion Welding" // International Conference on Extrusion and Benchmark, Bologna, Italy, 2011.pp.461.– 466.;
6. J. Kandis, H. Valberg; „Metal flow in two-hole extrusion of Al-alloys studied by FEA with experiments", European Scientific Association for Material Forming, Erlangen, April, Germany 2012.pp.493.- 498.

Structure and Volume of Thesis

The promotion paper is written in English, it consists of 4 chapters, conclusions, and the list of literature sources used, 53 figures, a total of 108 pages. The list of references has 66 information sources and 3 appendices.

1. BASIC CONCEPT OF PROBLEM

1.1. Extrusion

Extrusion (*extrusion – pushing out* from Latin) is formation of a material, pushing it through the extrusion die in order to obtain constructions of a certain profile. It is shown in Figure 1.1 that the raw material always is in the shape of a bar – a cylindrical aluminum block, which is heated in the induction cooker up to the temperature of 450–500 °C (depending on the aluminum series number). The heated bar is pushed through the extrusion die with a large force (depending on the temperature and dimensions of the specimen), giving a form to the profile.



FIGURE 1.1. Layouts of extrusion dies (a) and the material flow of billets in the extrusion die (b)

The length of profiles is usually from 25 to 45 meters – depending on the form and needs. As soon as the profile has left the extrusion die, it is cooled with air or water. In order to avoid formation of stress and to obtain a completely straight product, the profile is stretched prior to testing all important dimensions and quality of the surface.

If the initial parameters of the extrusion welding process are not set correctly, for example, a stable, constant temperature is not maintained, geometry of the extrusion die is not correct, the extrusion die is not cleaned from the accumulated deposits from the previous extrusion process in a quality way, the extrusion die is damaged, there is an insufficient quantity of the oiling substance, etc., then some individual parts of the extruded profile or the whole profile can have an insufficient quality of the extrusion welds.

In order to examine the processes taking place during the extrusion welding, there have been numerous researches carried out over the years. In 2002 a paper [52] was published, where the most important know-how on the extrusion welding throughout the 20th century was summarized. The early researches were mainly conducted by the means of experiments, nevertheless they facilitated to good understanding of the basic processes of extrusion welding, paying attention also to the extrusion welding, when the distribution of material flows takes place with the assistance of a web in the extrusion dies. Technologies for testing and inspecting joints are out-of-date, very expensive, time consuming and inaccurate.

During the 21st century, it was possible to study the metal flow in the FEM simulations [66, 60, 61, 63, 59, 58] with powerful and fast computers, as well as, using the powerful FEA programmes. Nowadays, within the framework of extrusion welding research, the FEA pays

the main attention to experimenting and studying the variable conditions in the extrusion welding chamber, when distribution of the metal flow with the assistance of the web takes place [7].

The extrusion welding process it is important to apply the correct conditions of the metal flow in the extrusion die in order to obtain the necessary pressure of the metal flow in the welding chamber, which would provide an adequate welding quality of joints. The most important conditions are sufficient heating of the billet's material, extrusion welding velocity and geometry of the extrusion dies. During the 21st century the attention was mainly focused on studies of the first two conditions.

1.2. Testing methods of extrusion welding joints in the extrusion process

The most common testing method to assess the quality of extrusion welding is a tensile test established by the European standard EN ISO 6892-1:2010 [23]. Specimens for the test are made according to the European standard EN ISO 2740:2009 [22]. Test specimens oriented in the direction orthogonal to the weld are prepared, and then stretched to fracture.

If failure occurs in the weld, the strength of the weld is evaluated from the yield stress or the tensile strength of the material as measured in the test, while ductility is evaluated from either elongation, or contraction of area of the test specimen at fracture. It is generally agreed upon that the ductility of the weld is a better measure of quality than strength, as welds with quite serious defects might have good strength. Defective welds therefore can be sorted out and scrapped based on ductility values if the specimen fractures in the weld.

Having examined several profiles of the extruded aluminum, we have come to conclusion that the ductility of deformation (change of the specimen's dimensions) is a better quality indicator than the tensile test, because during the course of experiment it was observed that due to a repeated crystallization of the specimen's metal, the material has a different solidity at different sections. Thus the specimen's material at different sections can have a less solidity than the joints originated during the extrusion process with the solidity of defects. In that way the tensile diagram does not provide information on the quality of joints originated at the time of extrusion welding. The low-grade joints can be better identified based on the deformation degree measurements. The deformation degree is determined according to the changes in the specimen's dimensions.

Deformation of the material in point of fact can be flexible, which disappears when the load is removed and the parts return to the initial state. The plastic deformation that remains, when the load is removed, starts when the impact of force is increased. This deformation – change of dimensions of the material are characterized by the deformation degree:

$$\varepsilon = \frac{\Delta l}{l} \cdot 100, \quad (1.1.)$$

where

ε – deformation ductility (%);

Δl – dimension of a specimen after tearing (mm);

l – dimension of a specimen before tearing (mm).

In order to determine the quality of a joint obtained as a result of extrusion welding, apart from the tensile test there are other static testing methods used, such as bending, torsion and other micro cracks inspection tests (micro analysis, study of the material structure, etc.).

Other static test methods than tensile testing has been used to determine weld quality in extrusion welding. Such methods are the bending test, the flattening test and various fracture mechanical tests. The quality of industrial extrusion welds is also commonly tested by expansion tests; a mandrel is then pressed into the open end of a hollow profile, or the

profile is expanded hydraulically. If the profile expands sufficiently before it fractures, this ensures acceptable ductility in the material and confirms that the profile does not contain serious defects. Expansion tests can be difficult to apply in some non-circular hollows, and in these cases flattening, or etching tests may be used instead.

For critical applications of light metals profiles with extrusion welds one can use fracture mechanics tests on samples taken from the profiles. In such tests a pre-crack is forced to propagate along the weld plane. Extrusion welds that behave satisfactorily in a tensile test may in a fracture mechanics test have reduced toughness compared to that of the parent metal away from the weld. In this case the welds usually have higher content of inclusions in the extrusion weld than outside it. The weld will thus represent a favorable plane for crack propagation compared to the locations away from the weld.

1.3. Defination of problem

If a crack is observed outside the area of a joint, it is considered that the quality of the extrusion welds is better than the quality of metal. But is it always true? Unfortunately, it is not always so. Figure 1.1 (a) shows a layout of an aluminum profile welded in the extrusion process, which is obtained from the aluminum profile with a joint in the middle of it, torn in the tension device. As it can be seen in Figure 1.2 (b) and (c), initially there are some micro cracks (two un-welded stripes with no metallic bond that extended along the length of the profile) observed in the area of the welds, which are indicative of a low-grade weld. The micro cracks have originated from an insufficient pressure in the weld chamber. It can be seen that the specimen breaks outside the low-grade extrusion welding area, despite the fact that there is a clearly visible defect in the joint. This example shows that the specimen with an extrusion joint can demonstrate a good result (i.e. the specimen does not break in the joint area) in the tensile test, even if the quality of the joint is not sufficient.

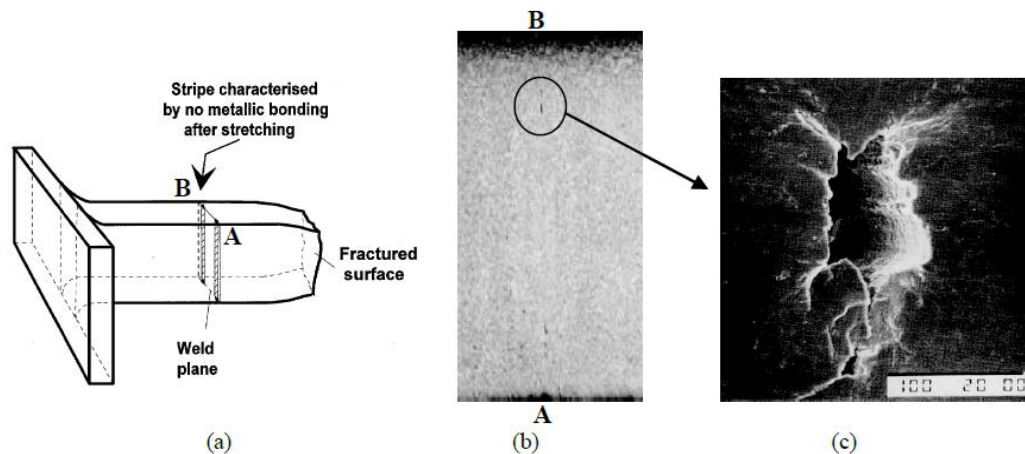


FIGURE 1.2. Specimen deformed in the tension device; (a) Specimen torn in two as a result of the tensile test; (b) Extrusion welded joint defect, and (c) Micro cracks in the joint area in magnification

Such a behavior of the specimen can be justified that as often as not the material is not of a similar solidity at all sections. During an extrusion process the billet and extrusion die are heated from outside up to the temperature of 500 degrees above zero, as a result there can be some temperature differences between the central part and outside, which harden differently during the process of precipitation hardening. As a result in the case seen in Figure 1.2, the material is softer away from the location of a weld then the extruded joints. When the tensile

test is performed, the softest area of the material starts deforming faster than the solid one or the extrusion welded area. The stress of the material in the incompletely welded section of the joint is not sufficient to identify the low-grade extrusion welds. When pulling is continued, the deformation localizes and grows in strength only in the already deformed section despite the fact that the material has significant faults in the adjacent extrusion welds area. As a result the low-grade extrusion weld is not identified.

Also this behavior is easily explained if the material away from the weld where the neck appears is softer than that in the weld zone itself. Upon stretching necking would then start in the softer region instead of in the hard weld zone. The degree of plasticization in the section of the specimen containing the defects would therefore not become so high that it would demonstrate the material weakness in reality present in this location. On continued stretching deformation would therefore be localized and would only take place in the neck, in spite of the presence of a serious material defect in the cross-section nearby.

In order to eliminate the shortages established in this chapter, an inspection method of the extrusion welded joints was developed, focusing the quality inspection directly on the locations of extrusion welds. The new testing method is based on the deformation measurements in the weld area and the result is described as a degree of deformation.

1.4. Conclusions

Considering the fact that there is a large probability that a break will originate outside the extrusion welding area, when the tensile tests of the aluminum specimen are performed, and frequently the quality of the welds joint area is better than the quality of metal, and that the material is heated not only from outside and a repeated process of precipitation hardening develops partly during the process, there is a need for more accurate tests to inspect the extruded welds.

In order to develop a simplified and accurate testing method focused on the extrusion welds, initially it is necessary to perform researches on deformations and behavior of the material, breaking them.

Being aware of the impact of temperature and speed on the quality of formation of welds, perform researches on the impact of geometry of the extrusion die on formation of the extrusion welding joints in the course of the thesis.

2. EXPERIMENTAL STUDY AND FEM-MODELLING OF SHEARING PROCESS

2.1. Introduction

The formation mechanism of the cut edge depends on whether the metal to be cut is soft or hard. While in sufficiently soft metals most of the cut surface is formed by shearing, in hard materials a greater portion of this surface is created by the metal undergoing fracture. Before the fracture is created across the section there is localised shear taking place in a layer inside the metal in the region between the upper and the lower shearing edge. In this article emphasis is on the mechanics of shearing taking place in this layer in soft aluminium alloys where the fractured part of the cut edge is either absent or represents a minor part of the cut cross-section.

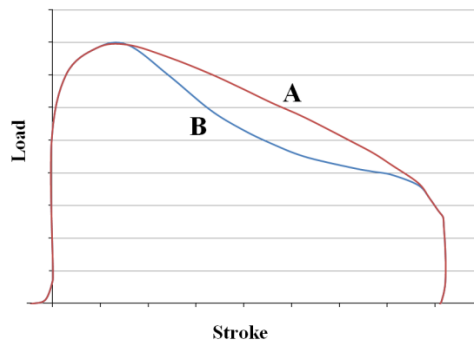


FIGURE 2.1. Principal sketch showing typical appearances of load-stroke curves in shearing.

A number of investigations into the mechanics in the deformation zone in shearing have been reported in the technical literature. Experimental work in which shearing was investigated by measurement of the load-stroke curve are for instance available in [4, 5, 9, 12]. The experiments were either performed in tensile test machines run in compression or in mechanical presses.

The measured load-stroke curve obtained for Al seems to have different appearance dependent on the test machine applied in the shearing process, see Fig.2.1. The load rises steeply in the beginning of the process then it flattens out after a while. As shearing continues it starts to decrease so that there is a distinct peak value of load. Behind the peak the declining part of the graph is approximately flat or it curves upward (A) or downward (B). Upward curvature is obtained when shearing is conducted in a tensile test machine [4, 5] and downward curvature when the process is set up in a mechanical press[5, 9, 12]. Since the new Extrusion Quality Test will be forced with punch, and for eksperimets will use mechanical presses, deformation is represented as a type (B) curve.

2.2. Experimental work

Axisymmetric experiments were performed in a mechanical press where four flat specimens of three different thicknesses were partially sheared with zero clearance between punch and shearing die. The initial thicknesses were 3.7 (Exp.no.1 and no.2), 5.6 (Exp.no.3) and 10.4mm (Exp.no.4) for the specimens used. The partial shearing depths of the specimens were 1.9, 3.5 and 8.3 mm. The punch and the die had sharp edges.

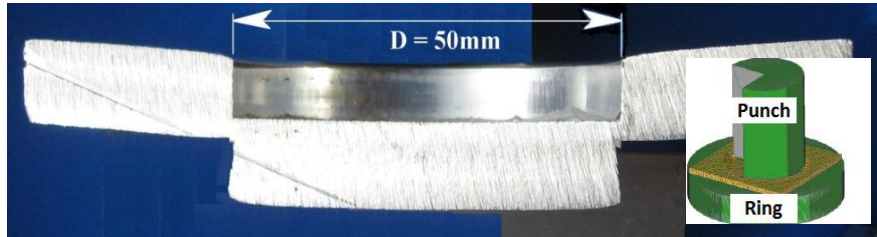


FIGURE 2.2. Section through the partially cut thick specimen.

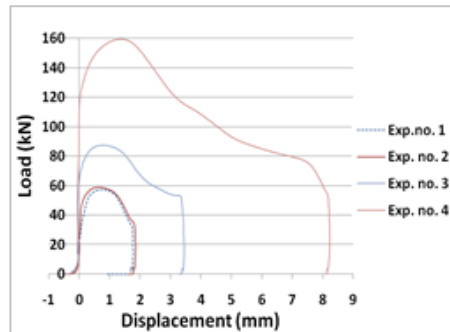


FIGURE 2.3. Load-stroke data from shearing experiments.

A photo of the cross-section cut through the thickest specimen is shown in Fig.2.2. Experimental shearing load on the punch was measured vs. the punch displacement. The recorded data are shown as graphs in Fig.2.3. As this figure shows the declining part of the curve behind the peak curved downwards; i.e. a B-type (see Fig.2.1) of load-stroke curve was obtained. Since shearing was done as partial shearing in a mechanical press the velocity varied throughout the stroke, being high in the beginning, then dropping down in a sinusoidal manner until it reached zero at the end of the partial cutting operation. For the thick specimen the velocity in the beginning was 20mms^{-1} .

2.3. FEM-model of the shearing process

A non-isothermal FEM-model was made to mimic the thick specimen shearing experiment using the software DEFORM-2D. Only a short description of the FEM-model is given here, for a full description see [8]. The model corresponded closely to Exp.no.4 with respect to geometrical and shearing conditions, as the real shearing speed was used in the model. A fine FEM-mesh was used in the workpiece material in the layer between the shearing edges to model the shearing process accurately.

The specimen was defined rigid-plastic with Coulomb friction ($\mu=0.1$). A special procedure was used to obtain flow stress data that gave the right simulated punch force. Starting point was the flow stress data given for the alloy Al99.7 in the DEFORM-2D data base.

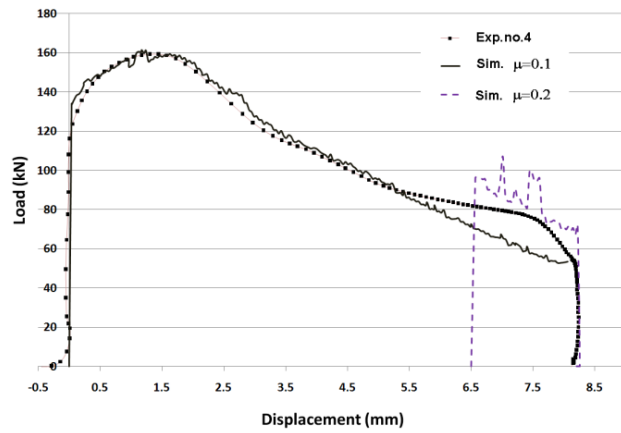


FIGURE 2.4. Comparison between load-stroke curve obtained in experiment and FEA.

2.4. Results of the FEA

Fig.2.4 shows an overlay plot of the load-stroke curve as obtained in the experiment and the corresponding FEM-simulation curve. As the figure depicts; with use of the modified flow stress data the experimental punch load response is predicted accurately by the model.

The modified model with constant 10mm s^{-1} downward punch velocity and 10mm s^{-1} upward velocity of the shearing die was also used for analysis. It corresponds to shearing with a stationary die and the punch moving downward with 20mm s^{-1} velocity. The advantage with this model is from a post-processing view because upon shearing the horizontal midline between the two shearing edges remains stationary.

The figures depict that early during shearing there is predicted a velocity gradient in a rather thick layer across the shear zone. As shearing progresses the layer with velocity gradient narrows down and shearing localizes in a thinner layer than before. The degree of shear localization can be quantified by the peak value of the velocity derivative vs. simulation step, see Fig.2.5. This parameter expresses the intensity of shearing in the layer. Fig.2.5 shows that this value is predicted to be low in the beginning. When shearing reaches a certain stage, i.e. simulation step 50 where 30% of a full cut has been obtained, however, this parameter start to increase. From now and onwards this parameter increases steadily until the full section has been sheared off.

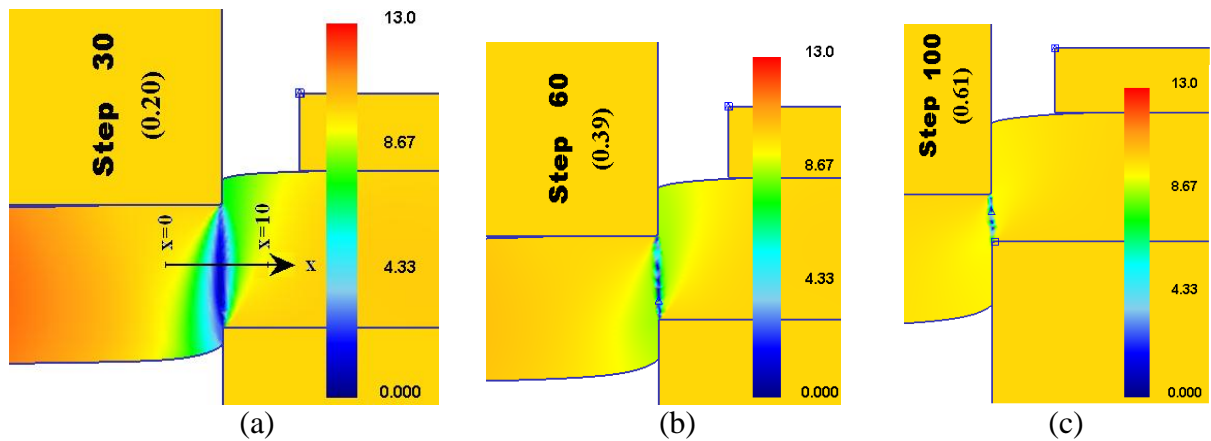


FIGURE 2.5. Velocity distribution in the shear zone at different stages of shearing. Numbers in parenthesis in this and following figures denote fraction of a full cut.

Even though a large number of scientific investigations have been conducted on the process of shearing (also named blanking) the situation is still one where the mechanisms of deformation in the process are not yet fully understood. Some early experimental investigations [6, 13] performed in the period 1950-70 revealed that in shearing of bars or blanks using sharp-edged dies, the mechanism of cutting was one where crack initiation can take place at each of the two approaching die edges rather early during shearing, so after the cracks have appeared the mechanism of partitioning will include crack growth across the thickness of the plate, instead of pure shearing over the full section. In some cases initiation and growth of the crack from the top edge of the die could be suppressed, then cracking would only occur from the bottom edge, see Fig.2.6.

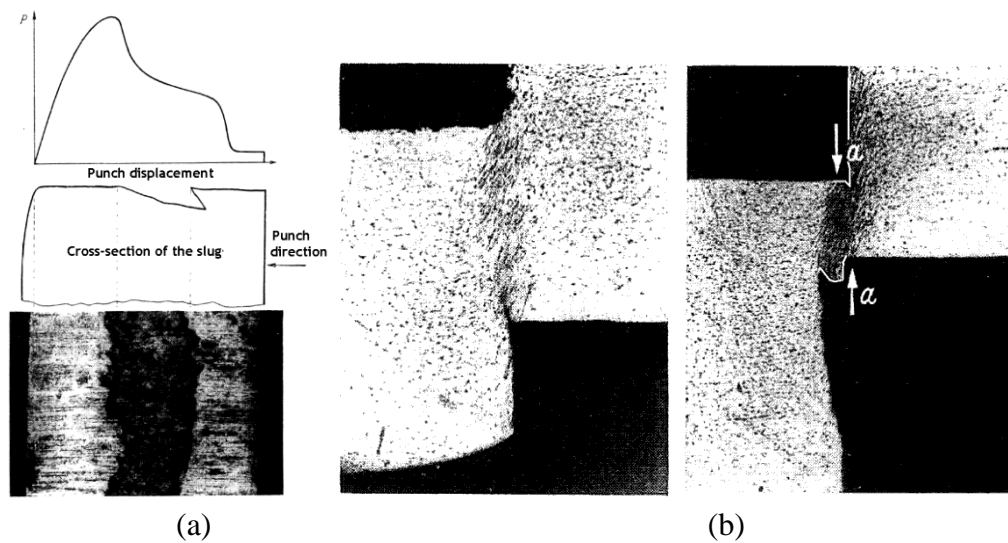


FIGURE 2.6. Shearing by crack growth from the cutting edges; (a) Load-stroke curve and appearance of sheared surfaces, (c) Cross-section through partially cut specimen at different stages of shearing [6].

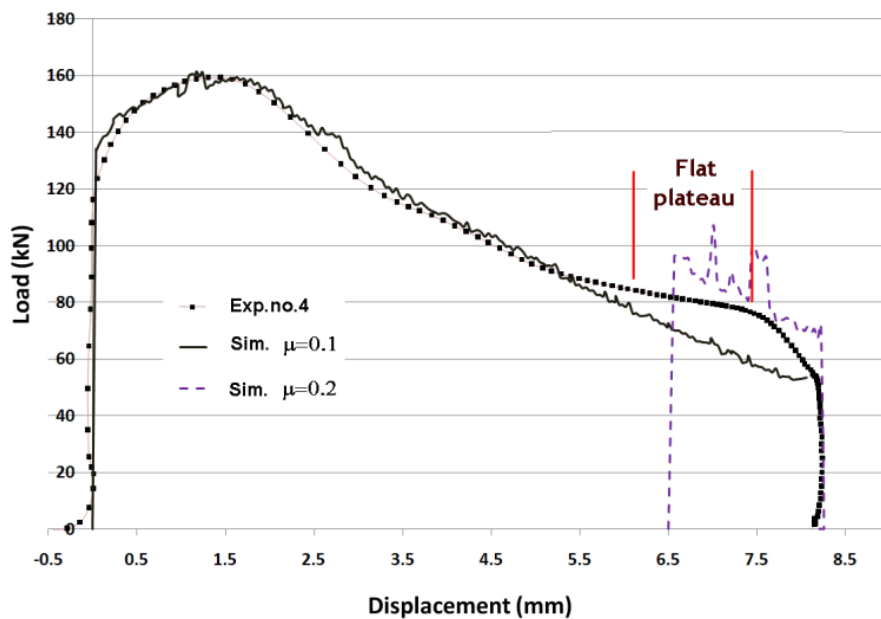


FIGURE 2.7. Load-stroke curve in shearing from experiment and FEM-simulations.

A special characteristic commonly observed in experimental investigations of shearing is that the measured load-stroke curve has approximately a flat plateau toward its tail end, see Fig.2.7. In an earlier investigation [11] we tried to FE-model the shearing process to study the conditions in the shear zone. When we modeled the process we assumed partitioning to take place by shearing only, i.e. without crack formation and crack growth. The model then predicted that the shear zone established over the thickness of the blank, extending from the top edge to the bottom counter-edge, would remain in the same location throughout the cutting operation. Moreover, prediction was that shearing would become more intense as cutting proceeded, so actually there would be strong shear localization in the shear zone.

Efforts aiming at getting the FE-model to reproduce the flat plateau near the end of the load-stroke curve were not successful at that occasion. The flat plateau did not occur in simulation unless we either assumed a strong thermal softening in the material, or a significant friction increase between dies and workpiece material towards the end of the stroke. When the flat plateau appeared both effects were exaggerated beyond what is realistic.

2.6. Conclusions

The mechanics of the shearing operation can be complex and hard to model by FEA. To be able to acquire accurate flow stress data from axisymmetric shearing experiments some conditions must be fulfilled. Friction between the shearing tool and the blank should preferably be eliminated. If the shear zone in reality moves laterally away from the plane extending between the shearing edges this must also be included in the FEA. Finally, the FEM-model must numerically be optimized to model the shearing process accurately.

Knowledge regarding the shear deformation in the internal shear zone in axisymmetric conventional shearing conducted on an Al-alloy can be obtained by FEM-analysis. In our analysis it was predicted that this zone remains rather thick, and without shear localization in the first 1/5th of the process. However, upon transition to the second stage the conditions changes as the shear zone starts to become thinner, concurrently as the shear intensity in it starts to increase. This trend continues throughout the last 3/5th of the process.

The shape of the load-stroke curve in shearing depends strongly on crack formation and crack growth. A crack that grows into the material reduces the remaining thickness of the blank, hence required shearing load decreases in relation to shearing without crack presence. When the crack halts, it becomes gradually pressed out of the shear zone by the advancing cutting punch. In this stage the remaining material thickness across the shear zone will not change much, and because of this there appears a flat plateau in the load-stroke curve towards end of shearing.

3. ANALYSIS OF GAS POCKET FORMATION DURING EXTRUSION OF AL PROFILES AND ESTABLISHING AN EXTRUSION SEAM WELD LIMIT

DIAGRAM

3.1. Introduction

One important mechanical characteristic of the extrusion process is the metal flow inside the material of the billet during the course of the extrusion process. The fact that metal flow is of great importance for the result in extrusion was confirmed by classical experimental work conducted in the early years of extrusion [7]. Then it was discovered that many of the common extrusion defects encountered in extrusion in fact are caused by metal flow phenomena, like for instance the formation of the defect commonly called pipe, towards the back end of the extruded rod.

Extrusion welding is shown in a Fig. 3.1. (a) and the flow of material through the form see Fig.3.1.(b). Hot or cold extrusion is the process by which a block of metal is forced through a die orifice under high pressure and is reduced in cross-section. Mostly, cylindrical bars or hollow tubes are produced this way but it is also possible to obtain complex shapes of products. However, products which can be produced by cold extrusion are relatively limited in size. If one considers axisymmetric forward extrusion, the main processing parameters which affect the resulting extrudate quality are; the press ratio, the die cone angle, the friction between the workpiece and the tooling, the mechanical properties of the material such as hardening and ductility characteristic, and the heating effects during forming. [7]

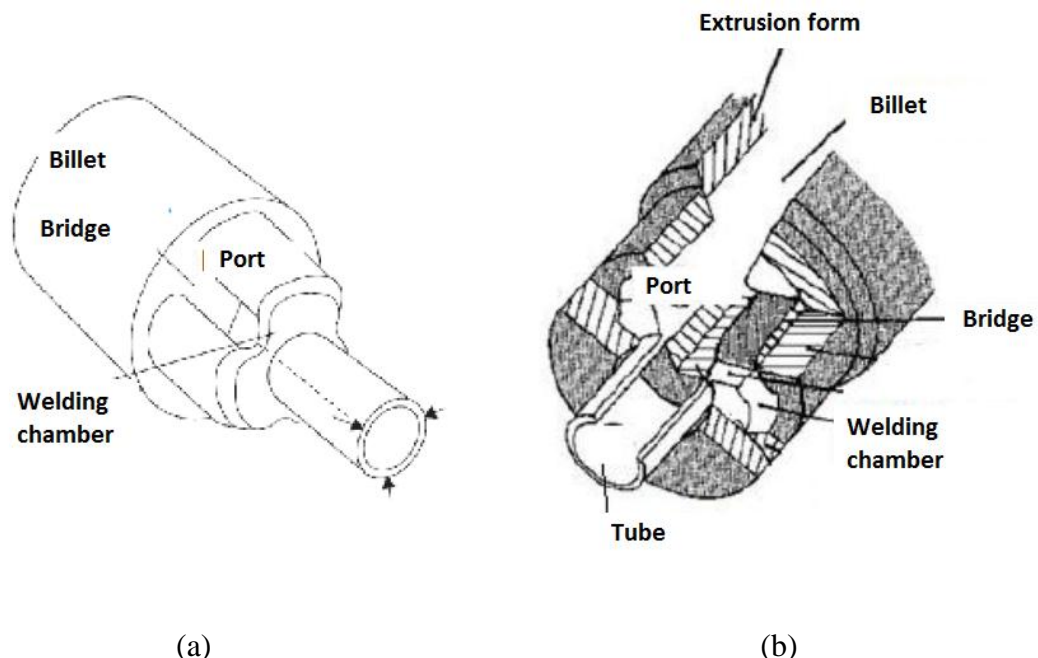


FIGURE 3.1. Extrusion welding (a) Material flow in hollow forward extrusion and (b) Extrusion form.

Friction affects not only the quality of the workpiece in metal forming but also the forming force. The force caused by friction depends on the lubrication conditions at the

interface between workpiece and container. Thus, one should investigate different lubrications when studying the forming processes. In combined FEA and experiments were used to obtain friction coefficients for cold forging processes like forward bar extrusion, forward tube extrusion and backward cup extrusion. A new friction testing method has been investigated assuming that the friction coefficient can be estimated without necessity of knowing the forming load and the flow stress of the workpiece. Using a realistic friction model a rigid-plastic FE-code was used in this work to investigate the friction distribution in the metal forming process. In axisymmetrical forward extrusion was studied both using a classical plasticity model with isotropic hardening and a nonclassical constitutive model.

The required force for the extrusion process is commonly considered to be composed of four additive parts represented by the formula:

$$F = F_{fc} + F_{dh} + F_{fd} + F_{ds} \quad (3.1.)$$

where,

F_{fc} - the force required to overcome the friction force against the container wall;

F_{dh} - the required force to overcome the deformational resistance to deform the metal homogeneously upon flow through the conical primary deformation zone in front of the die;

F_{fd} - the force required to overcome frictional resistance as the extrusion material in the primary deformation zone is sheared against the surrounding dead zone;

F_{ds} - the force required to shear-deform the material as it flows through the velocity discontinuities present at the entrance into the primary deformation zone and at the exit from this zone

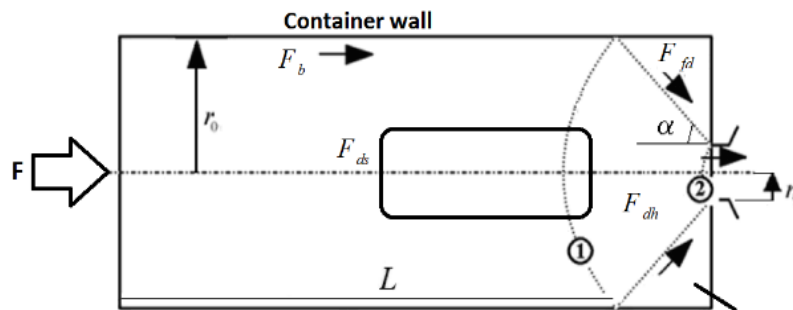


FIGURE 3.2. The total extrusion force is made up of four parts

In the literature it has been shown by theory how expressions can be deduced for each part of the force in eq.(3.1.). Then one arrives at the expression:

$$F = \underbrace{F_b}_{\tau \cdot 2\pi r_0 L} + \underbrace{F_{dh}}_{\pi r_0^2 \bar{\sigma} \ln \frac{r_0^2}{r_1^2}} + \underbrace{F_{fd}}_{\pi r_0^2 \frac{\tau_1}{\sin \alpha \cos \alpha} \ln \frac{r_0^2}{r_1^2}} + \underbrace{F_{ds}}_{2\tau_2 \pi r_0^2 \left(\frac{\alpha}{\sin^2 \alpha} - \cot \alpha \right)}, \quad (3.2)$$

where τ_1 is the friction shear stress against the tooling, τ_2 is the shear flow stress and σ the flow stress of the extrusion material. The other parameters used in the equation are shown in Fig.3.2.

To demonstrate the friction force of the overall outcome, involved two FEA. One of the cases was used lubricants, the other - completely dry friction. Results shown in Fig.3.3. It can be seen that the 2D simulate the outcome of the lubricants gives 3 times of the necessary force less than extrusion without lubrication.

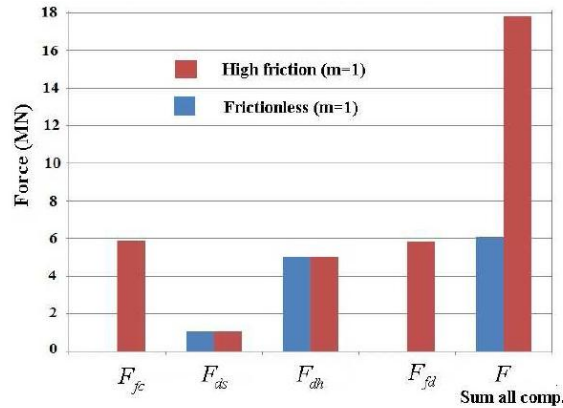


FIGURE 3.3. Theoretical load parts and total load

3.2. Finite Element Models

The finite element program DEFORM 2D® was used to simulate the pressure welding of metal in the extrusion process. A plane strain model was used in accordance with the extrusion models presented in applied metal forming. The model was built in half because of the symmetry. The work piece material was defined rigid-plastic while the tooling and die were set rigid. The bridge was modeled rectangular with rounded corners and the rear end of the bridge had always butt-ended shape. The flow stress data describing the plastic behavior of the alloy AA6082 has been expressed by a Zener-Hollomon equation presented in.

The initial temperature of the workpiece was set to 480°C and 420°C for the tooling. A frictionless plate was used in the weld chamber behind the bridge to prevent the profile from moving sideways over the midline. Two kinds of friction conditions between the workpiece material and the tooling were used to establish the extrusion seam weld limit diagrams, i.e. either it was used frictionless conditions or a state of very high friction.

3.3. The quality aspects of extrusion welding

However, with the availability of finite element codes, it is now possible and easy to evaluate the plastic flow of material in the welding chamber in fine detail. In this study various simulations have been run where the geometrical parameters of the welding chamber have been varied to see how the nature of metal flow behind the bridge will change.

In order to cover the variation in the behavior of material flow due to the geometrical changes in the welding chamber. The three geometrical parameters of the die used to make the triangle plot are the *width* of the porthole channel, the *height* of the weld chamber and the *thickness* of the extrusion as shown in Fig 1. Twenty four simulations, each based on different geometric measures, were run to study the characteristics of material flow through the welding chamber and particularly joining behind the bridge. It should be noted here that these simulations only deviated from those used to make the ESWL-diagram presented in the previous section with respect to friction conditions between tooling and extrusion metal. The ternary diagram is based on simulations in which a high-friction state was applied the ESWL-diagram was made for the frictionless case.

One should be aware that the importance of the concept of maintaining adequate interfacial welding pressure between the metal streams making the seam weld has been known for a long time. Akeret [1] not only suggested a critical pressure of at least three times the flow stress of extruding material but also proposed certain geometries of welding chamber to attain proper welding of metal streams. For the case of pothole extrusion he also pointed out that it is important to attain adequate metal flow into the gaps between the cores of the mandrel. To obtain proper metal feed in this location various combinations of the welding geometries should be tested.

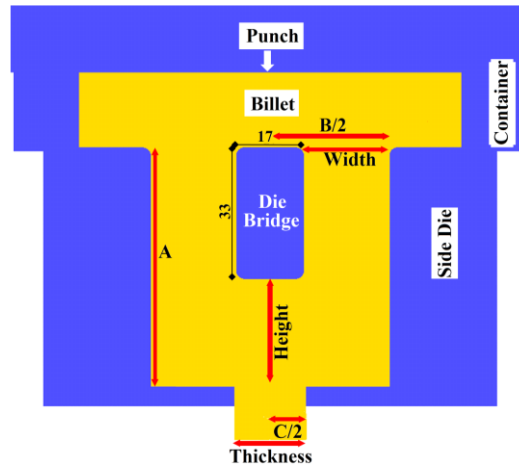


FIGURE 3.4. Geometrical condition in the 2D-extrusion models at start of simulation.

According to Akeret appropriate joining of the different material streams in the welding chamber require a sufficiently large welding chamber. When the welding chamber is too small the metal streams are not pressed completely into each other, and it is not possible to get a full profile section. When there is a wide welding chamber, one gets a dead zone behind the bridge. Sometimes in the welding chamber behind the bridge, a gas pocket may be observed. If this gas pocket forms, there will be weak extrusion seam quality in the final extruded profile. In case of extrusion of hard alloys aiming at optimum die strength, a narrow welding chamber would be favorable. But, on the other hand the welding chamber should be wide in order to obtain complete filling of metal and optimum pressure conditions upon seam welding. Valberg [14] used a particular extrusion geometry which gives a gas pocket behind the bridge and low pressure seam welding conditions. A small welding chamber size close to the critical size was chosen intentionally to obtain a gas pocket behind the bridge to investigate the conditions of seam welding with little feed of metal into the weld chamber.

Though the billet preheating and speed affect the flow distribution and also changes the temperature within the die, design of the die has significant affect on the yield in extrusion production [8]. In order to get strong welds in hollow section profiles various weld criteria has been considered to obtain rules for proper die design. The height and width of the welding chamber in relation to the die exit has been considered critical and main factors to provide good extrusion seam welds.

Many rules and criteria for seam welds quality evaluation have been considered. The first study was by Akeret who expressed the maximum pressure at the interface between two material flows as the discriminating parameter for material welding. Another criterion was proposed by Piwnik and Plata, and it uses as discriminating parameter the integral over time of the contact pressure, rated to the actual effective stress acting on the contact surface. Another criterion was expressed by Donati and Tomesani [3], which considers the velocity as

a correction factor, in order to reduce the influence of the dead zone below the web on the integral value.

However, with the availability of finite element codes, it is now possible [14] and easy to evaluate the plastic flow of material in the welding chamber in fine detail. In this study various simulations have been run where the geometrical parameters of the welding chamber have been varied to see how the nature of metal flow behind the bridge will change.

3.4. Finite Element Models

The finite element program DEFORM 2D® was used to simulate the pressure welding of metal in the extrusion process. A plane strain model was used in accordance with the extrusion models presented in applied metal forming. The model was built in half because of the symmetry. The work piece material was defined rigid-plastic while the tooling and die were set rigid. The bridge was modeled rectangular with rounded corners and the rear end of the bridge had always butt-ended shape. The flow stress data describing the plastic behavior of the alloy AA6082 has been expressed by a Zener-Hollomon equation presented in. The initial temperature of the workpiece was set to 480°C and 420°C for the tooling. A frictionless plate was used in the weld chamber behind the bridge to prevent the profile from moving sideways over the midline. Two kinds of friction conditions between the workpiece material and the tooling were used to establish the extrusion seam weld limit diagrams, i.e. either it was used frictionless conditions or a state of very high friction.

3.5. Material Flow in the Weld Chamber

The bridge divides the billet into two metal streams which join together behind the bridge in the weld chamber. The geometrical parameters of the welding chamber have significant effect on the material feed into the space behind the die, and how the extrusion material rejoins behind the bridge. There are three ways the material can join dependent on weld chamber geometry and amount of feed of metal into the space behind the bridge.

The FEA-predicted distribution of effective strain rate in the material around the bridge and in the weld chamber varies as the material flow changes in the direction from complete filling behind the bridge, to the presence of a void here, and finally to the situation where a stable gas pocket appears.

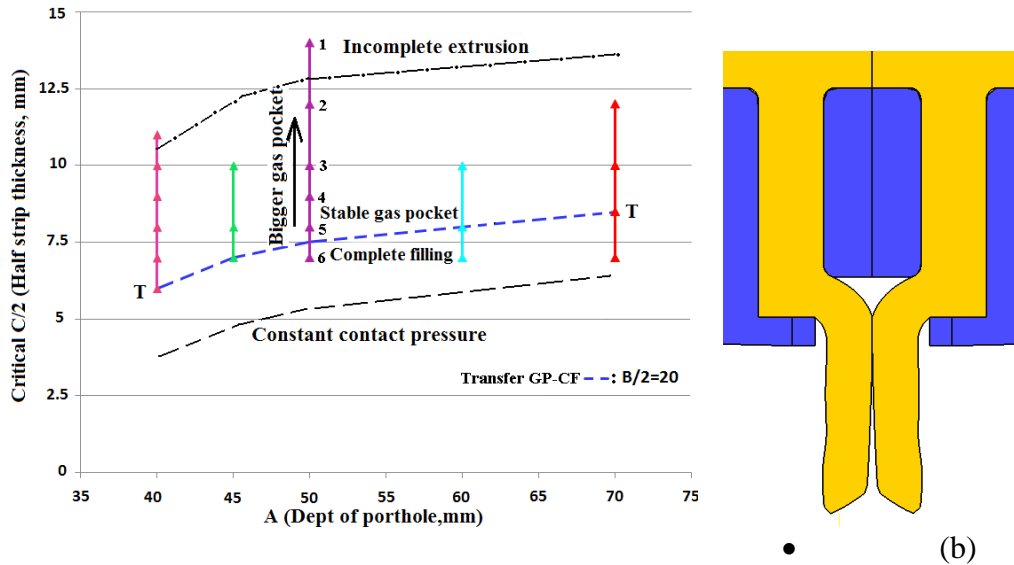


FIGURE 3.5. a) Identification of an ESWL-line for 2D extrusion seam welding and b) Situation where an incomplete extrusion is obtained.

3.6. Extrusion form geometrical effect of extrusion welding quality

The bridge divides the billet into two metal streams which join together behind the bridge in the weld chamber. The geometrical parameters of the welding chamber have significant effect on the material feed into the space behind the die, and how the extrusion material rejoins behind the bridge. There are three ways the material can join dependent on weld chamber geometry and amount of feed of metal into the space behind the bridge. This is visualized in Fig 3.5. by pictures taken from different FE-simulations of extrusion welding.

Simulation of the extrusion process for the case $B/2=20\text{mm}$ and $C/2=14\text{mm}$ with the die hole set equal to 14mm is represented in Fig.3.5. (a) by the point denoted 1. With this extrusion geometry the appearance of metal flow was as shown in Fig.3.5. (b), i.e. an incomplete extrusion was obtained. Knowing this fact a new simulation was run but this time with the die hole made a bit smaller, i.e. the parameter $C/2$ was set equal to 12mm . The new simulation is represented by the point denoted 2 in Fig 3a. With this new extrusion geometry, more feed of material into the space behind the bridge was predicted and complete extrusion was obtained. However, there was still not sufficient feed behind the bridge to avoid the formation of a stable gas pocket here. Three additional simulations represented by the points 3, 4 and 5 in Fig 3a were then run in which the die hole was reduced further in stepwise manner from 10 , to 9 and then to 8mm . In all three cases a stable gas pocket was predicted appearing behind the bridge, but the size of the pocket became smaller as the $C/2$ value was decreased.

Then a final simulation was run for the same extrusion geometry with $C/2$ reduced down to 6mm . The simulation showed that there was sufficient feed of metal into the weld chamber behind the die bridge to fill up the whole space here, and a situation of complete filling of the weld chamber had been obtained. Thus, by running of altogether six simulations we had confirmed that the nature of metal flow in this idealized 2D-extrusion welding die can be of three different categories. With a big die opening the metal flows through the weld chamber without being able to produce a complete cross section in the “extrusion”. Then, if the die opening is made smaller there is more feed into the weld chamber and a transition occurs to a state where a complete extrusion is formed, but a gas pocket will reside behind the bridge during the extrusion stroke. Finally, as the die hole is reduced further a new transition takes place and the weld chamber fills up completely with extrusion metal.

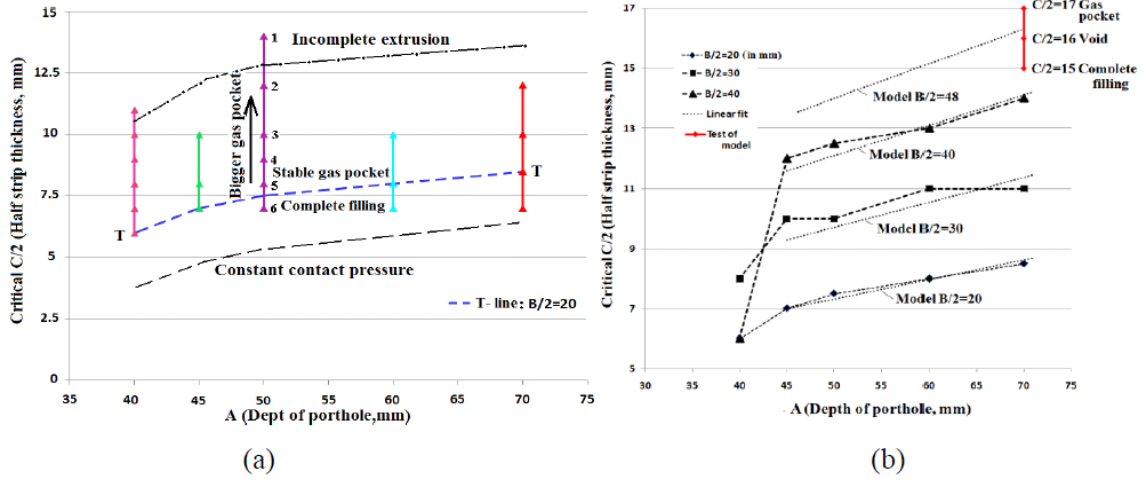


FIGURE 3.6.(a) Extrusion seam weld limit diagram (ESWLD) obtained by FEA of 2D extrusion welding. (b) ESWLD from FEA and predictions of our model.

Additional simulations were then run for different values of the porthole depth (A). Thus the transition point between extrusion causing complete filling of the die and a stable gas pocket was identified, see Fig. 3.6 (a), for multiple A-values. Now a line was drawn that connected all points by which there was this transition. Assuming that it is unfavorable to run extrusion seam welding with presence of a gas pocket behind the bridge, we have arrived at an extrusion seam weld limit

(ESWL) line for frictionless extrusion with $B/2=20$, and different values of the porthole height (A), represented by the line denoted T-T in Fig. 3.6 (a).

The same analysis, as that above for $B/2=20$ mm, was now repeated for $B/2=30$ mm and then for $B/2=40$ mm to obtain two additional ESWL-lines. In Fig.3.6 (b) all three lines obtained for the case of $B/2=20$, 30 and 40mm are plotted into what we will denote an extrusion seam weld limit diagram (ESWLD).

We chose to exclude the points for $A=40$ mm which represents a weld chamber of very small height, and then fitted each of the obtained ESWL-lines to the linear equation:

$$(C/2=aA+b) \quad (3.3)$$

A diagram was then made in which the constants a and b of the linear equations were plotted as a function of the B-value. From the graphs a linear fit was made for the constants:

$$b=0.1486B/2+1.0989 \text{ and } a=0.0018B/2+0.029 \quad (3.4)$$

This way we arrived at an equation for the critical dimension of the die hole, i.e. the parameter $C/2$, by which there is a transfer (as C is decreased), from a gas pocket being present behind the bridge to complete filling in this location:

$$\frac{C}{2} = \left(0,0018\frac{B}{2} + 0,029\right) A + 0,1486\frac{B}{2} + 1,0989 \quad (3.5.)$$

The prediction of the model for the case of a die where the porthole extends as far away from the midline of the process as the container does, i.e. an extrusion geometry where there is no ledge between the wall of the container and the die, is also shown in this figure. A series of simulation were now run for this situation and the depth of the porthole set equal to $A=70\text{mm}$ and $B/2$ equal to 48mm . For this geometry the model predicted $C/2$ to be equal to $15, 16$ and 17mm . When the simulation was run we found that it represented a situation where the gas pocket behind the bridge disappeared as the die opening was reduced further. These test simulations have also been shown in Fig.3.6. (b) where they appear at the top of and at right hand side of diagram.

3.7. Ternary Extrusion Seam Weld Limiting Diagram

Ternary extrusion seam weld limit diagram summarizing the behavior of metal flow behind the bridge.

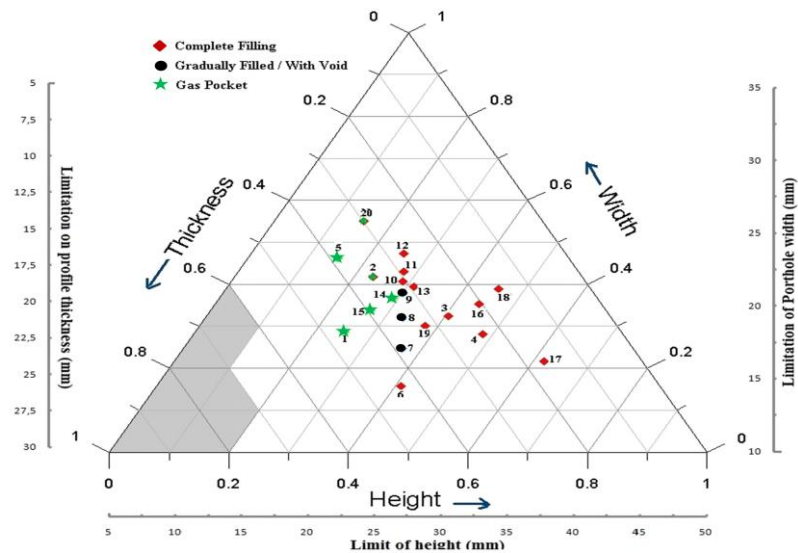


FIGURE 3.7. Ternary extrusion seam weld limit diagram summarizing the behavior of metal flow behind the bridge.

In order to cover the variation in the behavior of material flow due to the geometrical changes in the welding chamber, a ternary plot of FE-simulated data is shown in Fig. 3.7. The three geometrical parameters of the die used to make the triangle plot are the *width* of the porthole channel, the *height* of the weld chamber and the *thickness* of the extrusion. 20 simulations, each based on different geometric measures, were run to study the characteristics of material flow through the welding chamber and particularly joining behind the bridge. It should be noted here that these simulations only deviated from those used to make the ESWL-diagram presented in the previous section with respect to friction conditions between tooling and extrusion metal. The ternary diagram is based on simulations in which a high-friction state was applied the ESWL-diagram was made for the frictionless case.

Each of the three parameters of welding chamber geometry influences the behavior of metal flow. The minor changes in one of the parameters have significant impact on the way material flows; but it has always some contribution from the remaining parameters. All results obtained from the models have been plotted in the ternary graph. The ternary extrusion seam weld limiting diagram here shows the contribution of each geometrical parameter with respect to the nature of the metal deformations within the welding chamber. The graph is a Barycentric plot on the three variables; height, width and thickness which sum up to a constant (1 in this

case). The diagram graphically depicts the proportions of the height, width and thickness for one particular extrusion geometry as dots in the triangle. The dots have been distinguished according to the nature of material flow behind the bridge, whether there is a gas pocket or there is complete filling there. The position of the dots along with their separation according to these metal flow phenomena leads us to the regions within the diagram where behavior of metal flow can be predicted as the geometry of welding chamber changes.

Each simulation has been given a number and represented by a dot in the limiting diagram. All those simulation models, in which the region behind the bridge was completely filled by the material, have been marked with red color (◆). The black circular dots (●) present the simulation models where there is formation of a void behind the bridge or material slowly fills up the region during the course of extrusion. The green dots (*) show the presence of a gas pocket which remains till the end of extrusion stroke. It is important to notice that for the green points (*) the transition from one form of metal flow to the other is gradual.

It is important to notice that simulation models were made within limitations of geometrical measures, e.g. the width of the porthole cannot exceed the radius of the billet. Similarly there have been limitations on the maximum and minimum values of the profile thickness. The maximum height value has been taken as 14mm. While remaining within certain limiting values the results have been combined into the form of ternary extrusion seam welding limit diagram. The shaded areas of the diagram predict those regions of extreme geometrical combinations of weld chamber height, porthole width and profile thickness where the extrusion process or the product does not remain appropriate.

The trend of points with the green color (*) is towards the left side of the diagram marking a region of gas pocket formation. While most of the areas in the right bottom corner of diagram show complete filling behind the bridge.

3.8. Conclusions

Because of the availability of grid pattern experiments for two-hole extrusion it has been possible to confirm that metal flow predicted in our FEA-model is very close to real flow. This is especially true for the die with short distance between the holes. For the die with holes placed further apart from each other, there was more discrepancy between simulation and experiment. The peripheral shear zone in front of the die (and adjacent to the container wall) then appeared more localized in the experiment than in FEA.

The FEA reveals that the metal flow in front of the die changes strongly when the two holes in the die are moved sufficiently far apart from each other. With short die hole distance the main metal flow will be in the middle of the billet. With long distance between the die holes, however, the holes will appear close to the container wall, and the main metal flow ahead of the die will then be directed laterally away from the centre of the billet toward the container wall.

The analysis shows that the tested formula eq.(3.2) tends to overestimate calculated extrusion load highly because the formula for the load component due to friction on the conical dead zone ahead of the die is predicted much too high.

FEA applied on a case of idealized 2D porthole extrusion welding has helped to establish an *extrusion seam weld limit diagram* (ESWLD) to characterize the metal flow phenomena present behind the rear end of a die bridge, and to identify when there is a transfer from gas pocket formation here to a situation of complete filling.

The two types of diagrams, including the rather complicated ternary diagram, show when there can be expected a change in the nature of material flow and how the geometry of the extrusion die affects the occurring flow phenomena.

It is proposed to extend the concept to include prediction of seam weld pressure right behind the die bridge, so it can also be shown how the joining pressure are affected by the varying geometry of the portholes, the welding chamber and the profile thickness.

4. DETERMINING THE WELD QUALITY IN EXTRUSION WELDING

4.1. New innovative concept for testing of extrusion welds

The new test concept for determining the quality of extrusion welds is best explained by referring to Fig.4.1. In Fig.4.1. (a) a picture from a FEA-analysis of a simplified 2D extrusion process are shown in which two metal streams are joined by extrusion welding behind a bridge. In this case the conditions in the welding chamber were chosen so that the weld chamber behind the bridge did not fill completely up with metal, instead a stable gas pocket remained behind the bridge during the course of the extrusion process. Fig.4.1. (b) shows the obtained extrudate in such an experiment where a strip profile was extruded with an internal seam weld (EW) in the midplane of the strip (hatched lines), in which the weld extended over the full width (W) and length (L) of the profile.

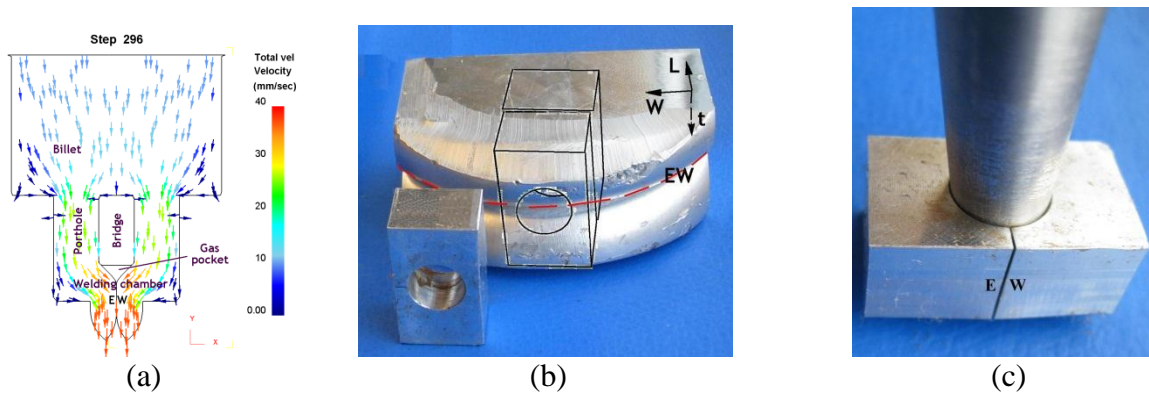


FIGURE 4.1. (a) Idealized 2D-extrusion with stable gas pocket behind bridge. Test technique; (b) Location of sample in profile with extrusion weld. (c) Mandrel expansion to specimen fractures.

In order to test one extrusion weld at a time by mandrel expansion a test specimen with a special geometry was designed, see the drawing shown in Fig.4.2. (a). The specimen was made as a small rectangular block with a round hole in the middle, and the hole was machined into the specimen at the location where the weld is present. Thus in mandrel expansion of the specimen it will fracture across the plane containing the weld. The actual strip profile that was tested in this case had dimensions $W=40\text{mm}$ and $t=10\text{mm}$, see Fig.4.1. (b).

Finally, Fig.4.1. (c) shows the situation after end of the mandrel expansion test performed on this specimen. The mandrel has been forced into the hole of the specimen, to a depth so that a crack has propagated across the thin section at one side of the specimen. As this plane was coincident with the seam weld of the extrusion, crack initiation and growth must have occurred along the weld plane in the specimen.

In Fig.4.1. (b) is shown how a number of specimens were prepared from the AA6082 strip profile (which was in a rather hard condition since it after extrusion had been stored for some years). The specimens were on purpose taken from a location near the front end and additional locations further backwards along the profile. The part of the profile that was tested represents the start up region of the extrusion process, during which conditions are non-stationary inside the die, before the metal flow becomes of steady-state nature. Because of this

it was thought that there might be variation in weld quality over this part of the extrusion. Specimens were taken from altogether three rows inside the profile, one row at one side (S1), one in the middle (M) and finally one row at the other side (S2) of the strip. With the exception of three specimens they were all expanded by a mandrel to fracture. This was done in a tensile test machine; the mandrel was gripped and held by one of the crossheads, while a plate was put on top of the other crosshead. A nut was laid on top of the plate as counter-die so that the tip of the mandrel coming out of hole of the specimen could move freely downwards into the hole of the nut.

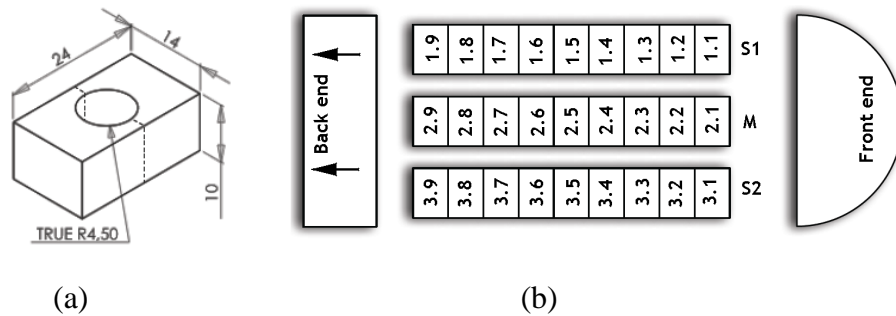


FIGURE 4.2. (a) Geometry of the new test specimen. (b) Location and numbering of specimens taken from the front end portion of the strip profile with an interior extrusion seam weld.

4.2. Summarization of results

During the test the load-displacement curve of the upper crosshead of the test machine was measured and recorded. When the specimen fractured at one side, see Fig.4.1. (c), the measured load dropped immediately down to zero. It was thus straightforward from this recording to determine the mandrel displacement length at the instant of specimen fracture. This parameter quantifies the ductility of the specimen tested in the expansion test.

4.3. Results analyze of weld testing

Load-stroke curves recorded in the expansion test specimens from the row S1 in the profile are shown in Fig. 4.3. (a). As the figure shows the load rose up very high in Exp.1.1 as no lubrication was applied between the mandrel and the specimen in this test. Since there was metal transfer from the specimen to the mandrel when the test was run under dry friction conditions, it was decided in continuation to perform the test in lubricated condition. In the next tests a lubricant was applied to the mandrel and inside the hole of the specimens. The required penetration load of the mandrel was now significantly reduced (by ~ a factor of 2) and the variation in load from one specimen to another one was rather small. All in all two types of load-stroke curves occurred; some with a smooth increasing trend, others with distinctive fluctuations in load. The first type of curves occur in cases where the lubrication is good so that sliding of the mandrel inside the specimen hole is smooth with even friction. The second type is most likely caused by lubricant breakdown so that contact is characterized by stick-slip fluctuations. The two types of behavior were observed to occur although the same lubricant was used, namely a commercial Cu-paste.

As shown in Fig.4.3. (a) a rapid drop in load was observed when the specimen fractured in the weld at one side of the hole, machined into the rectangular block. Hence, from

the load-stroke curve it is straightforward and fast to find the mandrel penetration depth into the hole at the instant of fracture. This parameter has been plotted in Fig.4.3. (b) for all specimens subjected to testing. In addition four reference specimens were made in which there were sound material without presence of any weld in the cross-section of the specimen where the hole is placed, and where fracture occurred.

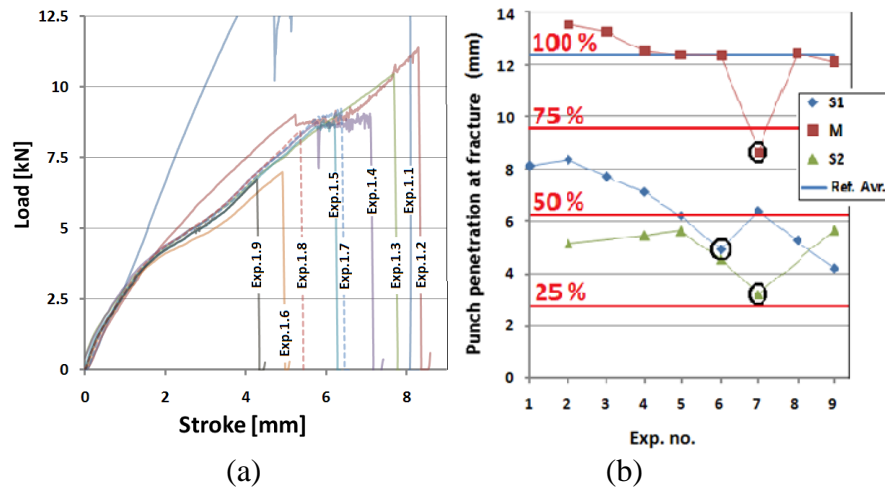


FIGURE 4.3. (a) Load-stroke curves recorded in mandrel testing of specimens from row S1. (b) Ductility data in terms of penetration depths for all tested specimens.

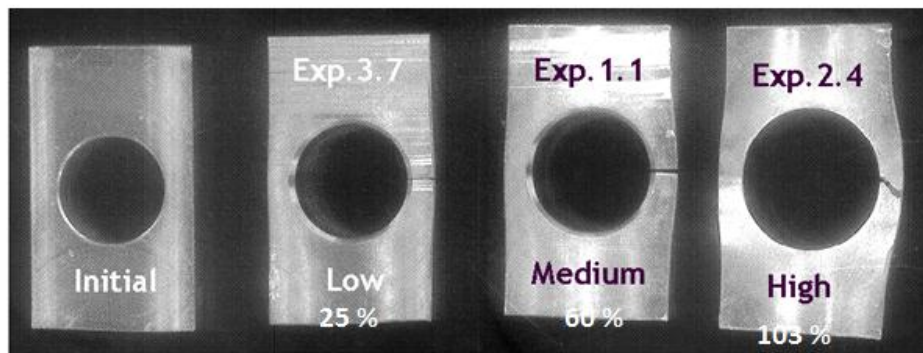


FIGURE 4.4. Initial specimen and specimens with different degrees of ductility.

As Fig. 4.3.(b) depicts there was a significant variance in the measured ductility between the different tested specimens. The punch penetration depth (PPD, in mm) at the instant of fracture of the weld can be divided in three classes for the different specimens. There was one class with low ductility (PPD=3-6, 25% - 50%), one with medium ductility (PPD=7-9; 50% - 65%) and one with high ductility (PPD=11-14; 98% - 106%). High ductility was experienced in the reference specimens without weld, and in all specimens from the row in the middle of the strip (M in Fig.4.3. (b)), with one exception, i.e. specimen 3.7. which had medium ductility. Medium ductility was also found in the specimens near the front end of the profile in row S1 at the side of the strip, while further behind in this row the specimens had low ductility. Finally, the ductility of all specimens taken from side row S2 was in the low regime.

As noted from Fig.4.3. (b) in all rows of specimens taken from the profile there was a decrease in ductility from the front end and backwards along the profile. In addition there was an even reduction in ductility along each row of specimens, with the exception of one measurement point at each row which had less ductility, so the even trend was broken, namely those measurements marked with circles in the Fig.4.3. (b). First thought was that this might be because of spread in behavior for the specimens, but since the low ductility value is observed to occur at approximately the same distance from the front end of the profile, it might be that this is a significant trend, and that the profile actually has less ductility at the location from which specimens numbered 1.6, 2.7 and 3.7 are taken.

4.3. The mechanics of the new test

To investigate the mechanical behavior of the test specimen upon mandrel expansion a FEM-model of the expansion test was build using the FEM-program DEFORM 3D.

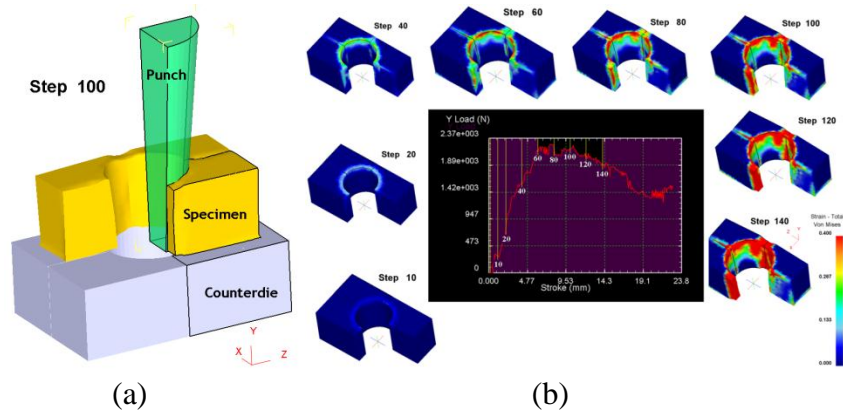


FIGURE 4.5. (a) FEM-model of mandrel expansion test, (b) Load-stroke curve plus deformation distribution (von Mises strain) in the test specimen from FEA at different stages of the expansion process.

One quarter of the process was modeled and a view of the model is shown in Fig.4.5. (a). In the simulation friction was described by a Tresca friction model in which the friction factor was set equal to $m=0.8$. The model was used to study how the test specimen is expected to deform plastically as the mandrel penetrates down into the hole of the specimen. It was also used to determine expected shape of the load-stroke curve in the test.

The predictions of the model is seen in Fig.4.5. (b) where the load-stroke curve is shown in the middle. The predicted deformations in the specimen at different stages of penetration of the mandrel are also shown by simulation pictures of the specimen placed around the curve. As this figure shows the load-stroke curve will increase until necking starts in the thin part of the specimen near the hole. Due to the necking phenomenon the load will reach a maximum value, and then will start to decrease. A thick specimen will deform by expansion caused by the mandrel, but in addition bending will be superimposed on the specimen in the location where it necks down. Because of this there is larger strain at the top side of the specimen than at the bottom.

4.4. Conclusions

While in the commonly used mandrel test a piece of the profile is expanded by forcing a mandrel into the hollow of the extruded profile, the new test is based on cutting a rectangular piece out from the profile wall so that the extrusion seam weld extends across the short mid-axis of the rectangle. A hole is then machined from the side into the middle of the rectangle, and the specimen obtained this way, is expanded by forcing a mandrel into the whole. This test specimen design secures highest strains in the thin part of the specimen which concurrently contains the seam weld. Reduced weld quality will therefore cause early fracture in the weld.

Specimen preparation in this test is easy and cheap, and it is also cheap to conduct the test. The test has been applied on a special profile with an extrusion seam weld. The test revealed that part of the weld was of bad quality because of a black contaminant film, probably lubrication, seeping into the weld during the extrusion process. In the mid-region of the welded profile where shiny Al-surfaces were joined together, however, the weld quality was good. Here the weld performed as good as the parent profile material outside the weld. Since the first try-out of the test gave so promising results, further application and try-out of the test is looked forward to.

CONCLUSIONS AND APPLICATION

1. In the course of the thesis it was concluded that:
 - 1.1. There can be cases, when, performing a tensile test of the extruded profile, a break will originate outside the joint area and the welded joints in the extrusion process will not be tested, although there are some micro cracks observed in the joint;
 - 1.2. There can be cases, when, under the influence of crystallization of metal, the quality of the welded joints with defects (micro cracks) is better than the quality of metal outside the joint area;
 - 1.3. Degree of deformation in the joint is a better quality indicator than the tensile test (coherence between the force applied to the specimen and volume of the deformation) for identification of defects in the extruded joints;
 - 1.4. Performing shearing experiments with an aluminum specimen:
 - 1.4.1. the shear zone becomes narrower and the material starts to become deformed, breaking, after transition to the second phase (~1/5 of thickness of the material used for the test);
 - 1.4.2. after ~3/5 of the process, the effect of the Plateau (a repeated increase of the load) is observed in the deformation curve, which originates when the billet material concentrates in the lower section of the shear course, thus creating tramps;
 - 1.5. Geometrical parameters of the extrusion die have an impact on the quality of extrusion welds;
 - 1.6. Some low-grade welded joints in the extrusion process can originate not only under the influence of speed and temperature, as it was considered up to now, but also depending on the geometry of extrusion dies;
 - 1.7. The new quality inspection method of the extruded aluminum welded joints permit much more accurate quality inspection measurements of the extruded joints if the measurements are performed to the welded joints instead of the whole profile.
2. Application:
 - 2.1. The geometrical limit diagram of extrusion die provides recommendations to manufacturers in selection of the geometry of extrusion die;
 - 2.2. The new quality inspection method of the extruded aluminum welded joints provides recommendations for improvement of the extrusion welding technology;
 - 2.3. The new quality inspection method of the extruded aluminum welded joints is universal – it can be also used to perform the quality inspection measurements of other metals.
3. There is a patent application submitted to the Norwegian Patent Office.

REFERENCES

1. Akeret R., "Extrusion Welds-quality aspects are now center stage". *5th Int. Al Extrusion Technology Seminar*, Vol. 1, 1992, pp.319.-336.
2. Ceretti E., L. and C. Kopsavilkumiardini, *Int. Conf. on Sustainable Manufacturing, Canada, 2008*. pp. 125.-132.
3. Ceretti E., Mazzone L., Giardini C., "Simulation of metal flow and welding prediction in porthole die extrusion: the influence of the geometrical parameters". *Int. J. Material Forming*, 2009, Vol. 2 Suppl. 1:101–104 DOI 10.1007/s12289-009-0494-9 © Springer/ESAFORM 2009.
4. Chang, T. M. : "Shearing of metal blanks", *J. of Inst. of Metals*, Vol. 78, 1950-51, pp.393-414.
5. Chang, T. M. and Swift, H. W.: "Shearing of metal bars", *J. of Inst. of Metals*, Vol. 78, 1950-51, pp.119.-146.
6. Chang T. M. and H. W. Swift, *J. of Inst. of Metals*, 78, 1950-51, pp. 119.-146.
7. Donati L., Tomesani L., "The prediction of seam welds quality in aluminum extrusion". *Journal of Materials Processing Technology*, 2004, pp. 153.–154 and pp.366.–373.
8. Donati L., Tomesani L., "The effect of die design on the production and seam weld quality of extruded aluminum profiles", *J. of Materials Processing Technology* , 2005, 164.–165 and pp.1025.–1031.
9. Timmerbeil, C.: "Untersuchung des Schneidvorgangs beim Blech", *Werkstattstechnik und Maschinenbau*, Vol.47, 1957, pp. 231.- 239 and pp. 350.- 356.
10. Kandis, J., Valberg, H. and Wu, W.: "Use of axisymmetric shearing as technological test method to gather flow stress and ductility data for metals", *ibid.*
11. Kandis J., H. Valberg and W. Wu, *Advances in Materials and Processing Technologies*, October 24th to 27th, Paris, 2010.
12. Krämer, W.: "Untersuchung über das Genauschneiden von Stahl und Nichteisenmetallen", *Ber. Inst. Umformtechnik, University of Stuttgart*, 1969.
13. Timmerbeil C., *Werkstattstechnik und Maschinenbau*, 47, Germany, 1957, pp. 231.- 239 and pp. 350.- 356.
14. Valberg H. S., "Applied metal forming; including FEM analysis". 1st Ed, Cambridge University Press, NY, USA, 2010.
15. Valberg H., *Int. J. of Materials & Product Technology*, 17, 2002, pp. 497.- 556.
16. Xianghong W. et al., *Materials Science and Engineering*, 2006, pp. 435.-436 and pp. 266.-274.
17. Støren S., Andersen L.: *Privāta komunikācija ar AS Hydro Aluminium un AS Bentelers*.